Arabian Journal of Chemistry (2015) xxx, xxx–xxx

King Saud University

Arabian Journal of Chemistry

www.ksu.edu.sa
www.sciencedirect.com

ORIGINAL ARTICLE

Green synthesis and biological activities of gold nanoparticles functionalized with *Salix alba*

Nazar Ul Islam [a,*], Kamran Jalil [b], Muhammad Shahid [a], Abdur Rauf [b], Naveed Muhammad [c], Ajmal Khan [d], Muhammad Raza Shah [e], Muhammad Atif Khan [f]

[a] *Department of Pharmacy, Sarhad University of Science and Information Technology, Peshawar, Pakistan*
[b] *Institute of Chemical Sciences, University of Peshawar, Peshawar, Pakistan*
[c] *Department of Pharmacy, Abdul Wali Khan University, Mardan, Pakistan*
[d] *Department of Chemistry, COMSATS Institute of Information Technology, Abbottabad, Pakistan*
[e] *HEJ Research Institute of Chemistry, ICCBS, University of Karachi, Karachi, Pakistan*
[f] *Centre of Biotechnology and Microbiology, University of Peshawar, Peshawar, Pakistan*

Received 7 April 2015; accepted 13 June 2015

KEYWORDS

Gold nanoparticles;
Salix alba;
Green synthesis;
Stability;
Biological activities

Abstract This study reports a facile and reproducible green extracellular synthetic route of highly stable gold nanoparticles. The aqueous gold ions when exposed to *Salix alba* L. leaves extract were bioreduced and resulted in the biosynthesis of gold nanoparticles (Au-WAs). The nanoparticles were characterized by UV–Visible spectroscopy (UV–Vis), Fourier transform infrared spectroscopy (FTIR), atomic force microscopy (AFM) and scanning electron microscopy (SEM). Their stability was evaluated against varying volumes of pH and sodium chloride as well as at elevated temperature along with enzymes inhibition, antibacterial, antifungal, anti-nociceptive, muscle relaxant and sedative activities. The UV–Vis spectra of the gold nanoparticles gave surface plasmon resonance at 540 nm while the AFM and SEM nanoparticles analyses revealed the particle size of 63 nm and 50–80 nm respectively. FTIR spectra confirmed the involvement of amines, amide and aromatic groups in capping and reduction of the gold nanoparticles. Au-WAs showed remarkable stability in different volumes of salt and various pH solutions however, Au-WAs were relatively unstable at elevated temperature. Au-WAs possessed good antifungal activity and showed significant antinociceptive

* Corresponding author. Tel.: +92 919331305.
E-mail addresses: islanaz@yahoo.com (N.U. Islam), organickami@yahoo.com (K. Jalil), shahidsalim_2002@hotmail.com (M. Shahid), mashaljcs@yahoo.com (A. Rauf), drnaveedrph@gmail.com (N. Muhammad), ajmalchemist@yahoo.com (A. Khan), raza_shahm@yahoo.com (M.R. Shah), atifkhan788@gmail.com (M.A. Khan).

Peer review under responsibility of King Saud University.

Production and hosting by Elsevier

http://dx.doi.org/10.1016/j.arabjc.2015.06.025

and muscle relaxant properties. These results revealed that the leaves extract of *S. alba* is a very good bio-reductant for the synthesis of gold nanoparticles that have potential for various biomedical and pharmaceutical applications.

1. Introduction

Metals nanoparticles especially gold and silver have attracted considerable attention in catalysis, optics, sensing, imaging and biomedical devices (Jain et al., 2008). Various physical and chemical processes have been used in the synthesis of nanoparticles; however these processes generate a large amount of hazardous byproducts (Thakkar et al., 2010). Green nanotechnology, that uses biological organisms, plant biomass or extracts is recently considered as an alternative to the conventional chemical and physical methods for the synthesis of nanoparticles in a clean, non-toxic, ecologically sound and environment friendly manner (Wang et al., 2009). The use of plant materials for the synthesis of nanoparticles could be more advantageous, because it does not require elaborate processes as various biomolecules like proteins, phenols and flavonoids in plants play a vital role in the reduction of silver or gold ions (Sathishkumar et al., 2012). In recent years, several plants are successfully used for efficient and rapid extracellular synthesis of stable dispersions of silver and gold nanoparticles (Kumar and Yadav, 2009).

Willow (*Salix alba* L.), (syn: white willow) belongs to the family Salicaceae and grows primarily on moist soils in cold and temperate regions (Klasnja et al., 2002). Traditionally, it has been used for the treatment of various ailments due to its potent antipyretic, analgesic and anti-inflammatory properties. The Assyrians and ancient Egyptians used the leaves and bark for musculoskeletal pain (Mahdi et al., 2006). The efficacy of this plant is mainly due to its phenolic contents and includes salicylates such as salicin (Fig. 1), which is a precursor of salicylic acid that played an important role in the development of aspirin (acetylsalicylic acid). Other phenolic compounds isolated from *S. alba* are flavonoids (e.g. quercetin) and tannins (Harbourne et al., 2009). Willow contains certain metabolites which act as tumor inhibitors by causing apoptosis and damages the DNA as well as affect the cell membranes or denature proteins in various human carcinoma cells (El-Shemy et al., 2007). Gold nanoparticles using the bark extract of *S. alba* have been reported to have high potential as colourimetric sensor for selective recognition and monitoring of cysteine among other amino acids (Bahram and Mohammadzadeh, 2014).

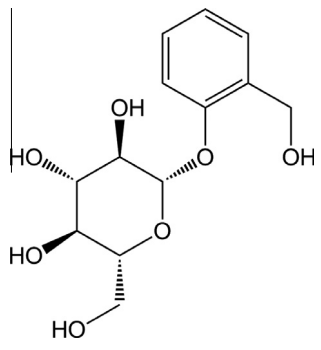

Figure 1 Chemical structure of salicin.

The present study reports the green synthesis of gold nanoparticles functionalized with the leaves extract of *S. alba* (Au-WAs). The gold nanoparticles were characterized with UV–Visible (UV–Vis), Fourier transform infra-red spectroscopy (FTIR), atomic force microscopy (AFM) and scanning electron microscopy (SEM). The effect of sodium chloride (NaCl), pH and reaction temperature on the stability of the biosynthesized gold nanoparticles was studied. Moreover, the gold nanoparticles were screened for various biological activities.

2. Materials and methods

2.1. Materials

Hydrogen tetrachloroaurate (III) trihydrate ($HAuCl_4.3H_2O$) obtained from Merck, was used as a source of Au^{III} ions. Leaves of *S. alba* were collected from Pishtakhara area of Peshawar, Pakistan. After identification by a taxonomist, a specimen was deposited with a voucher No. GDCH/001 in the herbarium of Government Degree College Hayatabad, Peshawar, Pakistan. The leaves were cleaned with distilled water, dried under shade and powdered. The powdered material (10 g) was put in a flask containing 100 ml of heated distilled water and stirred for 20 min on a hot plate. The extract was than filtered under vacuum and cooled immediately on ice.

2.2. Synthesis and characterization of gold nanoparticles

The effect of $HAuCl_4{\cdot}3H_2O$ concentration on the biosynthesis of gold nanoparticles was investigated by changing the volume of adding $HAuCl_4$ solution while keeping the volume of *S. alba* leaves extract constant. Different volumes of $HAuCl_4$ solution (1 mM) were added to the extract solution. After mixing the extract with aqueous $HAuCl_4{\cdot}3H_2O$ the color of solution rapidly changed to pink and then finally to ruby red, therefore indicating the reduction of gold ions to gold nanoparticles. The bioreduction of the $AuCl^{4-}$ ions was monitored by UV–Vis spectra of colloidal solution in 10 mm optical path length quartz cuvettes with a UV–Vis spectrophotometer (Hitachi U-3200, Japan) at a wavelength between 300 and 700 nm. Optimization was achieved using UV–Vis spectra at a ratio of 15:1 of gold-extract solution. The size of gold nanoparticles was characterized by AFM (Agilent Technologies 5500, USA) and SEM (JSM-5910-JEOL, Japan). For FTIR measurements, the bioreduced chloroauric solution was centrifuged at 10,000 rpm for 15 min to remove free proteins or other insoluble components. The samples were vacuum dried and were analyzed with an FTIR instrument (IRPrestige-21, Shimadzu, Japan).

2.3. Stability of gold nanoparticles

The effect of NaCl on the stability of gold nanoparticles of *S. alba* was studied by varying the volume (50–200 μl) of 0.1 M NaCl solution. In order to ascertain the pH effect on the stability of Au-WAs, the pH of the gold nanoparticles solutions was adjusted between 2 and 13 by drop wise addition of 1 M HCl or NaOH solutions. The effect of temperature on the stability of Au-WAs was determined by heating the gold nanoparticles for 30 min at 80 °C in a water bath.

2.4. Biological activities

2.4.1. Enzyme inhibition activities

Au-WAs along with an extract of *S. alba* were screened for enzyme inhibition activities against urease, xanthine oxidase and carbonic anhydrase-II enzymes.

For urease inhibition assay, the sample solutions were incubated with urea. Indophenol method was used to measure ammonia production as urease activity. Thiourea was used as the standard inhibitor (Sumi and Nippon Rinsho, 1996). The xanthine oxidase inhibitory activity of test samples was determined by measuring the rate of hydroxylation of the substrate (xanthine) and the subsequent formation of uric acid, which is a colorless end product of the reaction and showed absorption at 295 nm (Lee et al., 1998). The inhibitory activities of the test samples were compared with allopurinol, used as standard. Carbonic anhydrase-II inhibitory activity of the test samples was investigated using 4-nitrophenyl acetate, which is colorless. Upon hydrolysis it is converted to 4-nitrophenol and carbon dioxide. The formation of 4-nitrophenol, a yellow colored compound, was monitored during the experiment. The reaction was carried out at 25–28 °C. Acetazolamide was used as standard (Arslan, 2001). Experiments were performed in triplicate.

2.4.2. Antimicrobial activities

The antibacterial and antifungal activities were performed by using the well diffusion method (Boyanova et al., 2005; Uddin and Rauf, 2012) against bacterial strains of *Klebsiella pneumonia, Bacillus subtilis,* and *Staphylococcus aureus* and fungal strains of *Alternaria solani, Aspergillus niger,* and *Aspergillus flavus*. The bioassays were performed in triplicate.

2.4.3. Animals

BALB/c mice of either sex weighing 25–30 g and purchased from the National Institute of Health (NIH), Islamabad were used in the experiments. The animals were maintained in a 12 h light/dark cycle at 22 ± 2 °C for one week prior to experiments. Access to food and water was *ad libitum*. Experiments on animals were performed according to the NIH guidelines for the care and use of laboratory animals.

2.4.4. Acetic acid induced writhing test

The anti-nociceptive activity of Au-WAs was evaluated by acetic acid induced writhing assay in mice (Muhammad et al., 2012). All animals were withdrawn from food 2 h before the start of experiment. The animals were divided into six groups. Group I received normal saline and served as control. Group II was injected with standard diclofenac sodium (10 mg/kg, i.p). Group III and IV were injected with *S. alba* extract (CEW) at a dose of 50 and 100 mg/kg i.p respectively while group V and VI were treated with Au-WAs at corresponding doses of 5 and 10 mg/kg i.p. After 30 min of treatment, all animals were injected (i.p) with 1% acetic acid. The number of abdominal constrictions (writhes) was counted for 10 min after 5 min of acetic acid injection.

2.4.5. Muscle relaxant activity

The muscle relaxant activity of CEW and Au-WAs was evaluated by traction and chimney tests.

2.4.5.1. Traction test. In this procedure, the animals were exposed to a horizontal rubber coated metallic wire suspended about 30 cm in the air and rigidly supported with stands. The animals were screened after 30, 60 and 90 min of treatment with diazepam (0.25 mg/kg), normal saline (10 ml/kg), CEW (50 and 100 mg/kg, i.p) and Au-WAs (5 and 10 mg/kg, i.p). Each animal was hanged by hind legs from the wire and the time of hanging was recorded for 5 s. The failure to hang in less than five seconds was considered as the presence of muscle relaxant activity (Hosseinzadeh et al., 2003).

2.4.5.2. Chimney test. In this procedure, a 30 cm long Pyrex glass cylinder with an internal diameter of 3 cm and having a mark at 20 cm from its base was used (Muhammad et al., 2013). The animals were screened after 30, 60 and 90 min of treatment with diazepam (0.25 mg/kg), normal saline (10 ml/kg), CEW (50 and 100 mg/kg, i.p) and Au-WAs (5 and 10 mg/kg, i.p). Each animal was introduced at one end of the tube and allowed to move to the 20 cm mark from the base. When the animal reached the mark, the tube was moved immediately to a vertical position, the animal tried to climb the tube with a backward movement. The time required by each animal to climb backwards to the mark was noted. The mouse which failed to reach the mark within 30 s was considered with relaxed muscles.

2.4.6. Sedative activity

The apparatus used for this activity was consisted of an area of white wood (150 cm diameter) enclosed by stainless steel walls and divided into 19 squares by black lines. The open field was placed inside a light and sound attenuated room. Animals were acclimatized under red light (40 W red bulb) one hour before the start of experiment. After 30 min of treatment with diazepam (0.25 mg/kg), normal saline (10 ml/kg), CEW (50 and 100 mg/kg, i.p) and Au-WAs (5 and 10 mg/kg, i.p), each animal was placed in the center of the box and the numbers of lines crossed were counted (Archer, 1973; Goyal et al., 2009).

2.5. Statistical analysis

Data were expressed as mean ± standard error of the mean (SEM). For statistical analysis, ANOVA followed by Dunnett's post hoc test was used using GraphPad Prism 5 (GraphPad Software Inc. San Diego CA, USA).

Please cite this article in press as: Islam, N.U. et al., Green synthesis and biological activities of gold nanoparticles functionalized with *Salix alba*. Arabian Journal of Chemistry (2015), http://dx.doi.org/10.1016/j.arabjc.2015.06.025

3. Results

3.1. Characterization of gold nanoparticles

Gold-willow solutions were made in ratios of 8:1, 9:1, 10:1, 15:1 and 25:1. From the recorded UV–Vis spectra of Au-WAs, it was observed that by varying the volume of gold solutions while keeping the volume of the plant extract constant, a change in the intensity of UV–Vis spectra was observed (Fig. 2). The 15 ml of 1 mM gold solution and 1 ml of plant extract (i.e. 15:1) gave a uniform and sharp peak at 540 nm. As shown in the inset of Fig. 2, the change in peaks intensities can be correlated with change in color from purple blue to pink and then finally to ruby red. The appearance of ruby red color indicated the formation of gold nanoparticles in the solution. Further studies were conducted on the 15:1 gold-willow solution.

The AFM (Fig. 3) and SEM (Fig. 4) data revealed the average particle size of 63 nm and 50–80 nm respectively. The formation of gold nanoparticles was also confirmed by FTIR spectroscopy. FTIR spectra of both CEW and Au-WAs were recorded as shown in Fig. 5. FTIR spectrum of CEW has a broad peak at 3210 cm^{-1} suggesting the presence of OH group which may be responsible for the reduction of Au^{3+} to Au^{0} where as two bands of lower intensities at 2908 cm^{-1} and 2854 cm^{-1} indicated the presence of methylene group (CH_2) next to OH or NH_2 functional group. Similarly, bands at 1589 cm^{-1} and 1456 cm^{-1} show the C═C stretching of an aromatic ring which may indicate the presence of benzene ring, a band at very low intensity at 1660 cm^{-1} suggests the ortho substitution pattern of benzene ring and is supported by bands at 871 cm^{-1} and 748 cm^{-1}. Bands at 1361 cm^{-1} may be due to in plane bending vibration of OH of phenols, while the band at 1273 cm^{-1} is due to C—O stretching of phenol. These bands are shifted to higher absorption due to conjugation of oxygen with benzene ring. Similarly, spectrum of Au-WAs stabilized with *S. alba* leaves extract shows a band at 1242 cm^{-1} which correspond to —C—O—H groups while the bands at 1296 cm^{-1} and 1635 cm^{-1} correspond to amides of proteins.

3.2. Stability of gold nanoparticles

Fig. 6 shows a change in UV–Vis peak intensities with a corresponding color change due to the effect of varying pH on the stability of Au-WAs. The gold nanoparticles were quite stable in acidic medium; however, a gradual decrease in UV–Vis peak intensities showed less stability with an increase in pH of the colloidal solution. Similarly, in acidic pH, the solutions retained their characteristic ruby red color, however a deviation from this color was observed as the pH becomes alkaline. Peak broadening and red shift were noted at pH 12 and 13.

The effect of salt on the stability of Au-WAs was determined at different volumes of 0.1 M NaCl (Fig. 7). A gradual change of 0.1 M NaCl from 50 to 200 µl has little effect on the peak intensities of Au-WAs except for a decrease in their absorbance. At 250 and 300 µl, Au-WAs exhibited extreme peak broadening, therefore suggesting an aggregation of gold nanoparticles. As shown in the inset of Fig. 7, Au-WAs showed a color change from ruby red with a gradual change in the volume of 0.1 M NaCl solution.

Fig. 8 shows the effect of temperature on the stability of Au-WAs. An extreme peak broadening with red shift and a decrease in absorbance were observed after heating Au-WAs for 30 min at 80 °C. This indicates an aggregation of gold nanoparticles after heating the colloidal solution and can be confirmed from the SEM images as shown in Fig. 9.

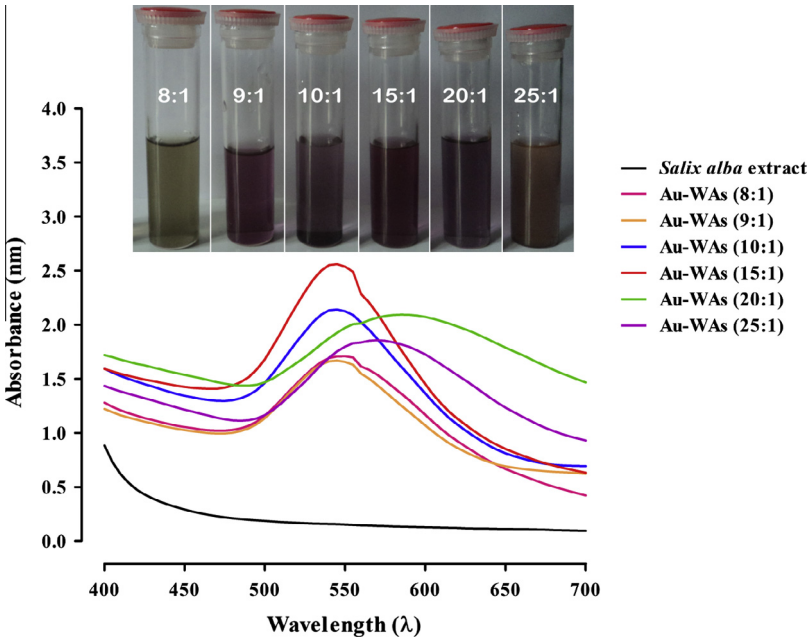

Figure 2 UV–Vis spectra of gold nanoparticles synthesized using different volumes of $HAuCl_4$ solution while keeping the concentration of *Salix alba* leaves extract constant. The inset photo shows the change in color with varying ratios of gold-extract solutions correspond to their absorption spectra.

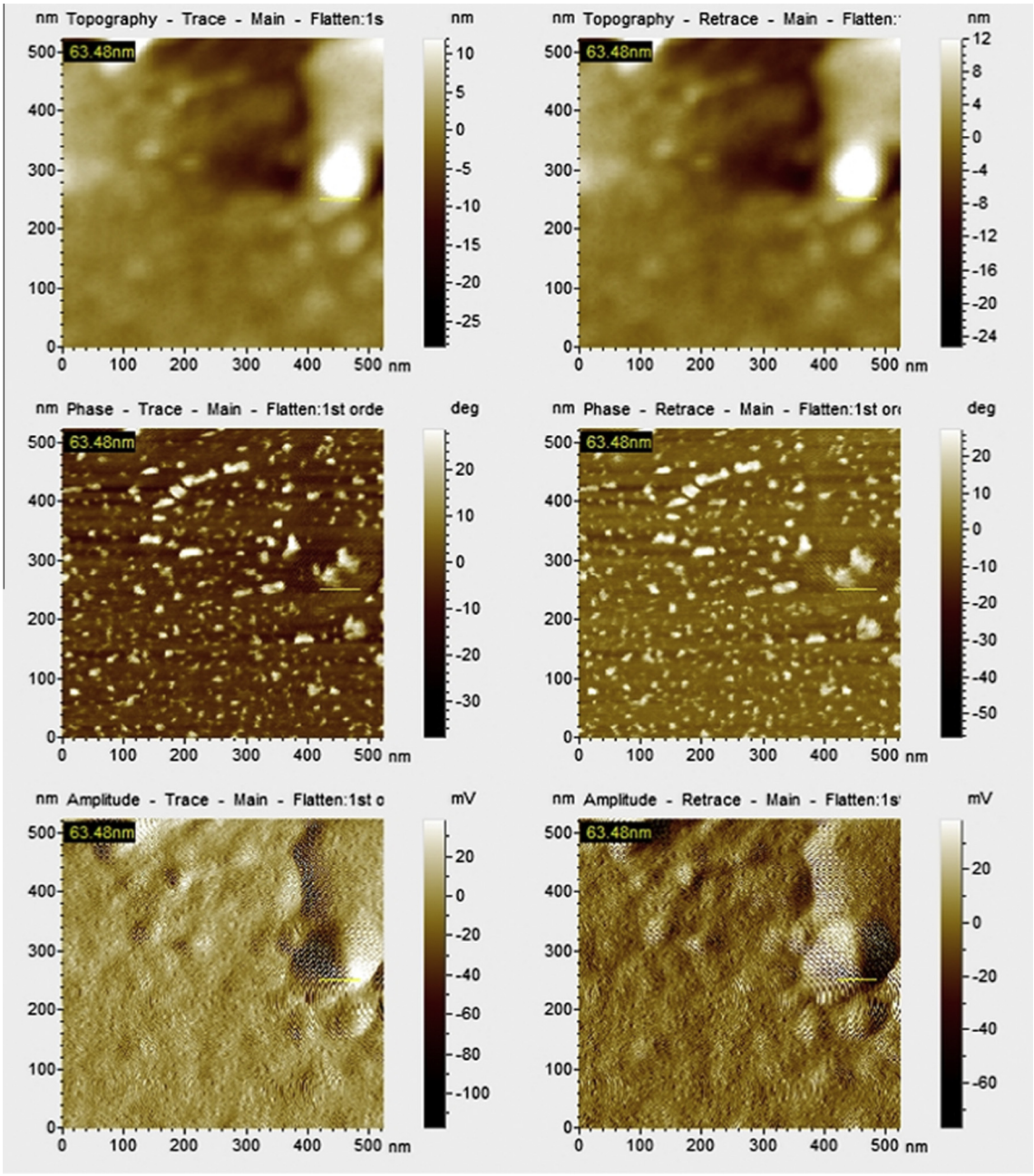

Figure 3 Atomic force microscopy images of optimized *Salix alba* gold nanoparticles.

3.3. Enzyme inhibition assays

As compared to the standard, CEW showed moderate inhibition against xanthine oxidase (22.1 ± 0.46) and carbonic anhydrase (22.1 ± 0.37) while low activity against urease (15.1 ± 0.77). Au-WAs were found inactive against xanthine oxidase; however, good activity was observed against urease (33 ± 0.37) and a low activity toward carbonic anhydrase (5.5 ± 0.26). The enzyme inhibition activities of CEW and Au-WAs against urease, xanthine oxidase and carbonic anhydrase are shown in Tables 1–3 respectively.

3.4. Antimicrobial activities

Au-WAs were tested for antibacterial and antifungal activities against *K. pneumonia, B. subtilis*, *S. aureus* and *A. solani, A. niger*, *A. flavus* respectively. As compared to the standard, CEW showed moderate antibacterial activity against the three bacterial strains while it was found inactive against the three fungal strains. Au-WAs possessed good antibacterial activity only against *S. aureus*; however, significant antifungal activity was exhibited by Au-WAs against *A. solani* and *A. niger* while low activity against *A. flavus*. The antibacterial and antifungal activities are shown in Tables 4 and 5 respectively.

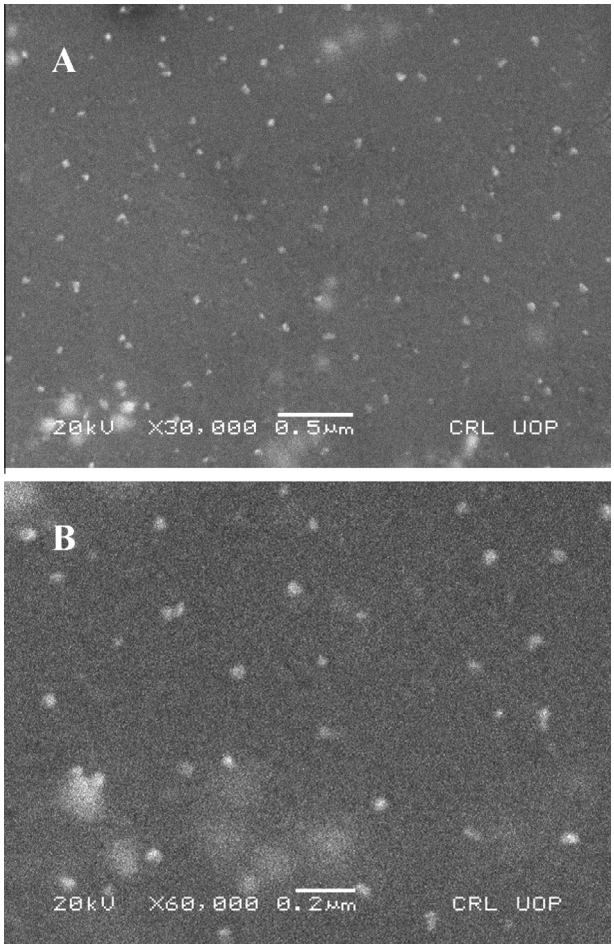

Figure 4 Scanning electron microscopy (SEM) images of optimized *Salix alba* gold nanoparticles at different resolutions (A and B).

3.5. Acetic acid induced writhing test

As shown in Fig. 10, CEW and Au-WAs at the tested doses possessed significant ($P < 0.001$) antinociceptive activity. A dose dependant effect was observed for both CEW and Au-WAs. The percent analgesic effect of CEW was 66.45% at 50 mg/kg while it was 78.98% at 100 mg/kg. Similarly the percent attenuation of acetic acid induced writhing for Au-WAs was 72.87% and 80.76% at doses of 5 and 10 mg/kg respectively.

3.6. Muscle relaxant effect

Table 6 shows the muscle relaxant effect of CEW and Au-WAs. After 20 min, in both chimney and traction tests, CEW at 50 and 100 mg/kg produced significant ($P < 0.05$) muscle relaxation. Similarly significant ($P < 0.05$) relaxant effect was demonstrated by Au-WAs at 5 and 10 mg/kg in the traction test however, in chimney test the effect was more pronounced at 10 mg/kg ($P < 0.01$). Moreover, after 30 and 90 min, all the doses of CEW and Au-WAs produced maximum muscle relaxation ($P < 0.01$) in both chimney and traction tests. In comparison, the standard diazepam at a dose of 0.25 mg/kg produced significant ($P < 0.01$) muscle relaxation after 30, 60 and 90 min in both tests.

3.7. Sedative effect

No sedative effect was exhibited by either CEW or Au-WAs, as the number of lines crossed was not significantly different from the saline group. In comparison, the standard diazepam produced significant ($P < 0.001$) reduction in the locomotor activity (Table 7).

4. Discussion

The synthesis and characterization of nanoparticles and their applications represent a rapidly growing concept and an emerging trend in science and technology (Gupta and Gupta, 2005). The use of plant materials for the synthesis of nanoparticles could be more advantageous, because it does not require elaborate processes (Song and Kim, 2009). In this study, gold nanoparticles were efficiently synthesized using the leaves extract of *S. alba*. The reaction between gold ions and *S. alba* extract was monitored by color change and UV–Vis absorption spectra. When a leaf extract solution of *S. alba* was added to 1 mM $HAuCl_4 \cdot 3H_2O$ solution, the color of solution changed from golden yellow to crimson red and then finally to ruby red at an optimized ratio of 15:1 (15 ml of 1 mM gold solution and 1 ml of *S. alba* leaves extract). The appearance of ruddiness color is indicative of formation of colloidal gold nanoparticles in the medium. Gold nanoparticles exhibit a ruby red color in aqueous media due to excitation of surface plasmon vibrations in the metal nanoparticles which give rise to surface plasmon resonance band centered at about 536 nm (Jensen et al., 2000). The plasmon resonance can be pictured as a "wave" of electrons sloshing over the surface of a metal nanoparticle. As a result, an enhanced electromagnetic field at and near the metal nanoparticle surface is set up. The position of the plasmon band (extinction spectrum) is best measured on a conventional UV–Visible spectrophotometer, and appears as a band with extremely high extinction coefficients (Murphy et al., 2008). In this study, it was observed from the UV–Vis spectra that the sharpness of absorption peak was dependent on the volume ratio of extract, thus being sharper with a higher ratio. No peak at a wavelength of 540 nm appeared for the *S. alba* extract however, in comparison, the gold nanoparticles functionalized with *S. alba* extract gave uniform and sharp peaks with varying intensities. It was noticed that the 15:1 ratio of gold solution and leaves extract in the reaction mixture is effective for the generation of gold nanoparticles as the UV–Vis peak becomes sharper and has maximum absorbance with SEM measured particle size ranging between 50 and 80 nm, which is in good agreement with the AFM analysis particle size measurement i.e. 64 nm. The UV–Vis spectra of Au-NPs at other ratios i.e. 8:1, 9:1, 10:1, 20:1 and 25:1 are either having lower intensities or exhibit broad peaks with red shifts at a wavelength corresponding to the plasmon resonance of gold nanoparticles (540 nm). This might be due to formation of large anisotropic particles or aggregation of nanoparticles in the medium. The surface plasmon resonance absorbance is extremely sensitive to the nature, size and shapes of the particles formed and their inter-particle distances (Sun and Xia, 2002). The size and concentration of gold nanoparticles can

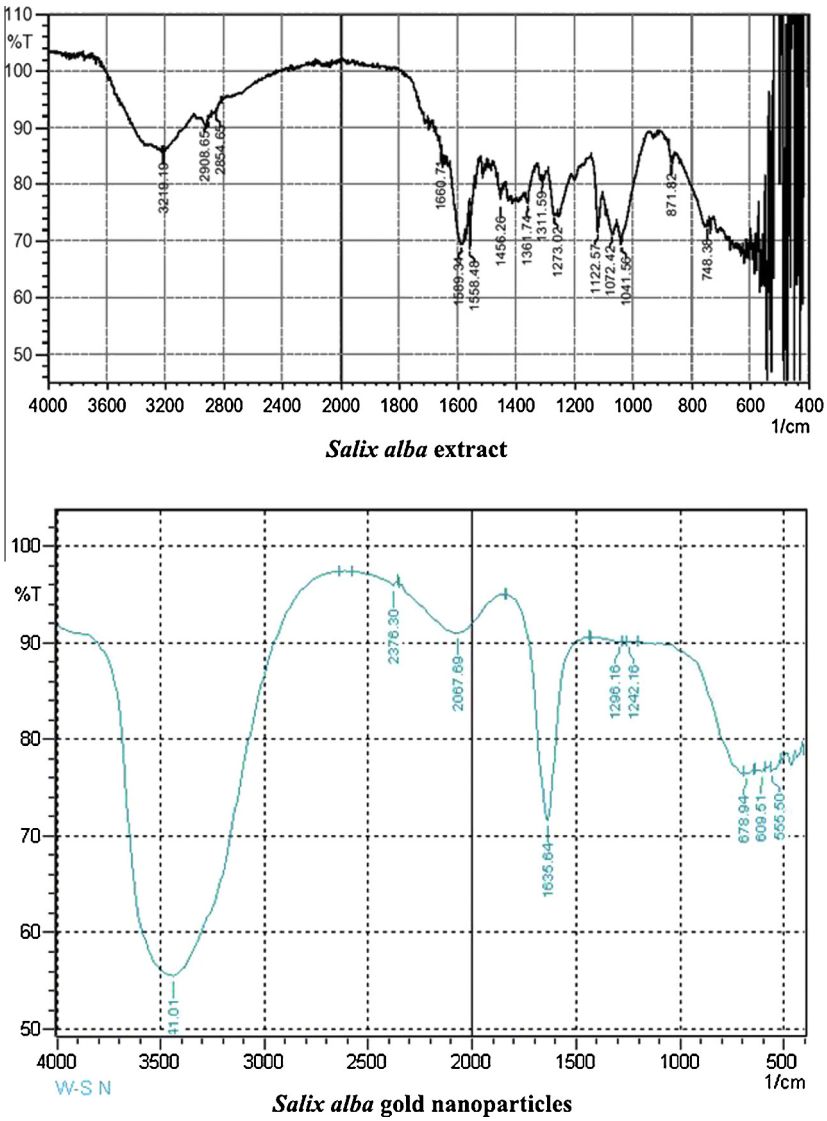

Figure 5 FTIR spectra of *Salix alba* leaves extract and its gold nanoparticles.

be determined directly from the UV–Vis spectra (Haiss et al., 2007; Murphy et al., 2008). Furthermore, the frequency of the plasmon band will differ from that of the simple isolated sphere if the nanoparticle is nonspherical in shape, and if it is close to other particles. Moreover, aggregation of noble metal nanoparticles red-shifts and broadens the plasmon bands (Murphy et al., 2008).

FTIR spectroscopic studies were carried out to investigate the possible capping and bio-reducing functional groups present in the extract. The FTIR spectrum of *S. alba* leaves extract shows absorption bands at 3210 cm^{-1} (—OH or —NH_2), 2908 cm^{-1} and 2854 cm^{-1} (—CH_2), 1589 cm^{-1} and 1456 cm^{-1} (C═C stretching of an aromatic ring), 1361 cm^{-1} (bending vibration of OH of phenols) and 1273 cm^{-1} (C—O stretching). Likewise the FTIR spectrum of gold nanoparticles shows absorption bands at 1242 cm^{-1} (—C—O—H), 1296 cm^{-1} and 1635 cm^{-1} that correspond to amide bands of proteins. This indicates that the gold nanoparticles synthesized using *S. alba* extract are surrounded by some proteins and metabolites having functional groups of amines, alcohols, ketones, aldehydes, and carboxylic acids. *S. alba* contains flavonoids like quercetin and tannis however, the major phenolic contents present is salicin. All these compounds contribute to the metal ion reduction processes and also stabilized the gold nanoparticles. The presence of salicin may be responsible for the formation of gold nanoparticles as this compound have hydroxyl group and glucosidal linkages which helps in the reduction of Au^{3+} to Au^0 (Villanueva-Ibáñez et al., 2015). Flavanones could be adsorbed on the surface of metal nanoparticles, possibly by interaction through carbonyl groups or π-electrons in the absence of other strong ligating agents in sufficient concentration (Shankar et al., 2004). Moreover, proteins could possibly form a coat covering the gold nanoparticles, thus preventing agglomeration of the particles and provide stability in the medium (Nel et al., 2009).

Synthesis of stable nanoparticles is an important aspect of nanotechnology as the stability of nanoparticles plays an important role in modulating their biological properties

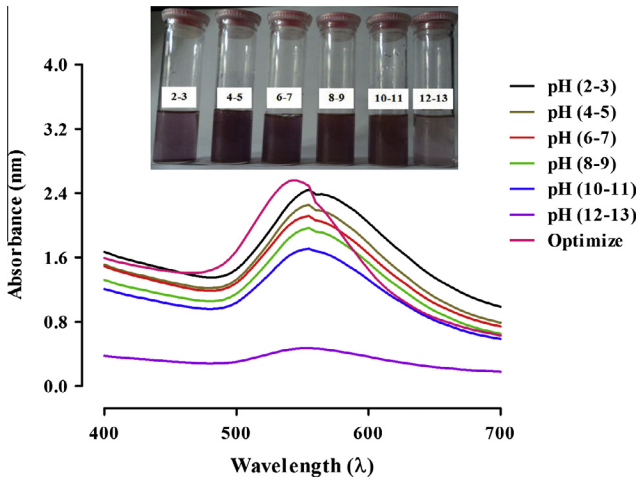

Figure 6 UV–Vis spectra showing the effect of varying pH on stability of *Salix alba* gold nanoparticles. The inset photo shows the change in color with different pH correspond to absorption spectra of the gold nanoparticles.

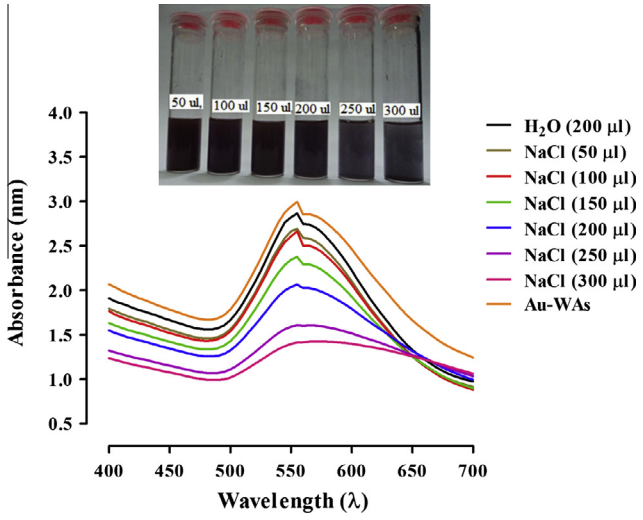

Figure 7 UV–Vis spectra showing the effect of different volumes of 0.1 M NaCl on stability of the gold nanoparticles. The inset photo shows the change in color of gold nanoparticles solutions with varying salt volume correspond to their absorption spectra.

(Gupta and Gupta, 2005). A reduction in stability can leads to total or partial loss of their nanoscale properties which may alters their cellular uptake and modifies their bioavailability and toxicity (Zhu et al., 2012). The most relevant processes that govern the stability and mobility of nanoparticles in the biological environment are agglomeration, aggregation, dispersion, sedimentation, and dissolution. These processes are dependent on the particle physicochemical properties that in turn are influenced by environmental parameters such as pH, temperature, ionic strength and presence of ligands or natural organic matter (Stankus et al., 2010; Levard et al., 2012). In this study, UV–Vis spectroscopy was used to efficiently evaluate the stability of gold nanoparticles. It was observed that the UV–Vis absorption spectra were significantly dependent on the

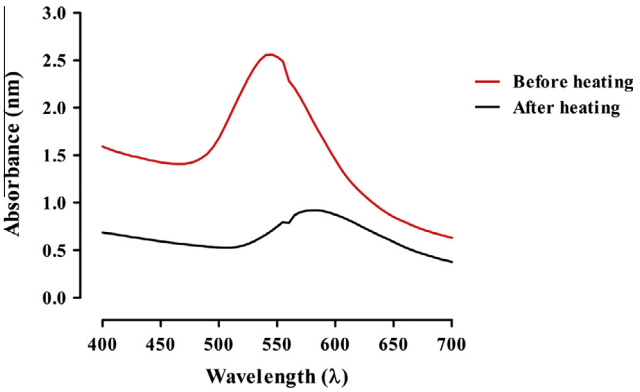

Figure 8 UV–Vis spectra showing the effect of temperature on stability of the gold nanoparticles before and after heating at 80 °C for 30 min.

size of gold nanoparticles with an increase in diameter, produced a dramatic red shift in their absorption spectra which might be due to shortening of distance or aggregation of gold nanoparticles. The gold nanoparticles were quite stable in pH range of 2–11 as there is almost no change in their UV–Vis spectra. This indicates their strong stability against either certain acidic or alkaline environments. The effects of NaCl concentration on the stability of gold nanoparticles were studied by using 0.1 M NaCl in quantities of 50–300 µl. It was observed from the UV–Vis absorption spectra that the *S. alba* mediated gold nanoparticles were relatively stable when the volume of salt increased from 50 µl to 200 µl. Their stability against varying volumes of salt can also be confirmed from the corresponding color of the gold nanoparticles solutions. Temperature is one of the important environmental factors that influence the stability, activity and chemical characteristics of materials (Vorkapic and Matsoukas, 1998). The effect of temperature on the stability of gold nanoparticles was investigated by heating the nanoparticles at 80 °C for 30 min. An increase in temperature facilitated aggregation of gold nanoparticles was observed as evidenced from the SEM images however, the gold nanoparticles still showed the typical plasmon resonance peak but with a red shift. Colloidal stability of nanoparticles is desired in most of the biological applications and in several other analytical applications (Dykman and Khlebtsov, 2012). Hence, understanding the stability under a wide range of environmental conditions, such as high salt concentration, extremes of pH, high temperature and buffer solutions is essential, which likely exhibits the fate of nanoparticles. The enhanced stability toward varying pH, ionic strength and temperature will enable us to explore different formulations of *S. alba* gold nanoparticles for potentially effective and safe therapy.

Considerable efforts are being made to develop and implement eco-friendly technologies for production of herbal based consumer products for providing better healthcare solutions (Chauhan et al., 2012). Gold and silver are frequently used for the synthesis of stable dispersions of nanoparticles using the extracts of herbs or other medicinal plants (Sadowski, 2010). In this study, the biosynthesized gold nanoparticles although devoid of antibacterial activity, showed excellent antifungal activity against *A. solani, A. niger* and *A. flavus*, while in comparison the *S. alba* extract was found to have

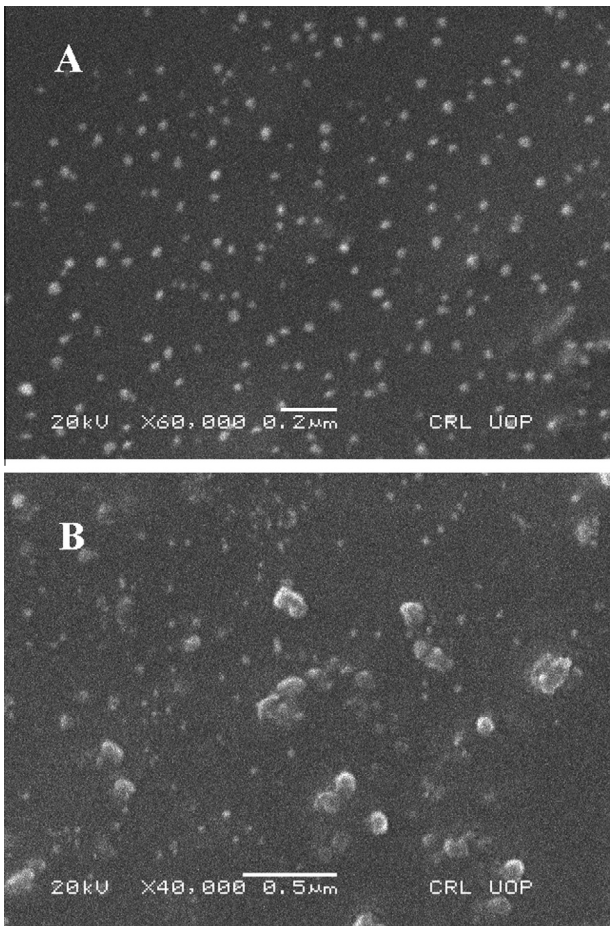

Figure 9 Scanning electron microscopy (SEM) images showing the effect of temperature on stability of the gold nanoparticles before (A) and after (B) heating at 80 °C for 30 min.

Table 1 Urease inhibition activity of *Salix alba* extract (CEW) and its gold nanoparticles (Au-WAs).

Sample	Concentration (mg/ml)	Inhibition (%)	IC_{50} ± S.EM (μg/ml)
CEW	0.2	15.1 ± 0.77	–
Au-WAs	0.2	33 ± 0.37	–
Thiourea	0.2	98.2 ± 0.15	21 ± 0.11

Values are expressed as mean ± SEM of three different experiments.

Table 2 Xanthine oxidase inhibition activity of *Salix alba* extract (CEW) and its gold nanoparticles (Au-WAs).

Sample	Concentration (mM)	Inhibition (%)	IC_{50} ± S.EM (μg/ml)
CEW	0.25	22.1 ± 0.46	
Au-WAs	0.25	NA	
Allopurinol	0.25	98 ± 0.16	0.59 ± 0.12

Values are expressed as mean ± SEM of three different experiments. NA = not active.

Table 3 Carbonic anhydrase II inhibition activity of *Salix alba* extract (CEW) and its gold nanoparticles (Au-WAs).

Sample	Concentration (mM)	Inhibition (%)	IC_{50} ± S.EM (μg/ml)
CEW	0.25	22.1 ± 0.37	–
Au-WAs	0.25	5.5 ± 0.26	–
Acetazolamide	0.25	89 ± 0.20	14 ± 0.11

Values are expressed as mean ± SEM of three different experiments. NA = not active.

Table 4 Antibacterial assay of *Salix alba* extract (CEW) and its gold nanoparticles (Au-WAs) (zone of inhibition in millimeter).

Samples	*Klebsiella pneumonia*	*Bacillus subtilis*	*Staphylococcus aureus*
CEW	12 ± 0.50	10 ± 0.67	12 ± 0.44
Au-WAs	NA	NA	10 ± 0.58
DMSO (negative control)	NA	NA	NA
Streptomycin	28 ± 0.20	30 ± 0.22	28 ± 0.24

Values are expressed as mean ± SEM of three different experiments. NA = not active.

Table 5 Antifungal assay of *Salix alba* extract (CEW) and its gold nanoparticles (Au-WAs) (zone of inhibition in millimeter).

Sample	*Alternaria solani*	*Aspergillus niger*	*Aspergillus flavus*
CEW	NA	NA	NA
Au-WAs	40 ± 0.45	50 ± 0.53	10 ± 0.56
Miconazole	100 ± 0.19	100 ± 0.22	100 ± 0.20

Values are expressed as mean ± SEM of three different experiments. NA = not active.

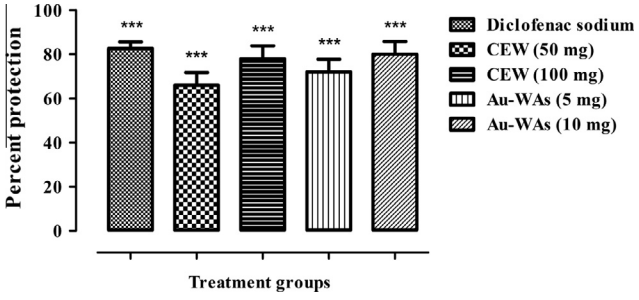

Figure 10 Percent antinociceptive effect of *Salix alba* extract (CEW) and its gold nanoparticles (Au-WAs). Each bar represents mean ± S.E.M for a group of six animals. ANOVA followed by Dunnett's post hoc test. $^{*}P < 0.05$ and $^{**}P < 0.01$ as compared to saline treated control group.

Table 6 Effect of *Salix alba* extract (CEW) and its gold nanoparticles (Au-WAs) on muscle relaxation (chimney test and traction test).

Group	Dose (mg/kg)	Chimney test (%)			Traction test (%)		
		30 min	60 min	90 min	30 min	60 min	90 min
Diazepam	0.25	100 ± 0.00**	100 ± 0.00**	100 ± 0.00**	100 ± 0.00**	100 ± 0.00**	100 ± 0.00**
CEW	50	33.65 ± 2.00*	50.78 ± 1.77**	50.09 ± 1.06**	35.22 ± 02.87*	55.98 ± 1.90**	55.00 ± 2.11**
	100	35.98 ± 2.98*	53.22 ± 1.76**	52.99 ± 2.65**	35.98 ± 1.02*	56.81 ± 2.00**	55.90 ± 2.19**
Au-WAs	5	38.01 ± 2.90*	48.09 ± 1.87**	48.00 ± 1.77**	37.09 ± 0.23*	47.90 ± 3.00**	47.88 ± 2.09**
	10	50.08 ± 2.76**	58.98 ± 1.88**	58.80 ± 2.01**	39.89 ± 1.99*	60.01 ± 2.00**	59.70 ± 1.99**

Data presented as mean ± S.E.M, (n = 6). ANOVA followed by Dunnett's post hoc test.
* $P < 0.05$.
** $P < 0.01$ as compared to saline treated control group.

Table 7 Effect of *Salix alba* extract (CEW) and its gold nanoparticles (Au-WAs) on locomotor activity.

Treatment	Dose	Number of lines crossed in 10 min
Saline	10 ml/kg	134.98 ± 0.98
CEW	50 mg/kg	135.76 ± 5.09
	100 mg/kg	134.87 ± 1.98
Au-WAs	5 mg/kg	127.45 ± 2.06
	10 mg/kg	128.54 ± 6.09
Diazepam	0.25 mg/kg	15.87 ± 0.87***

Data expressed as mean ± S.E.M, (n = 6). ANOVA followed by Dunnett's post hoc test.
*** $P < 0.01$ as compared to saline treated control group.

moderate antibacterial activity but was inactive against these fungal strains. Gold nanoparticles possess well developed surface chemistry, chemical stability and a large surface to volume ratio due to which more number of drug molecules gets adsorbed on their surfaces via electrostatic attraction between the amine groups of drugs and nanoparticles. The gold nanoparticles surrounded by a number of drug moieties now act as a single group against the microbial organisms thereby increasing the microbial activity (Burygin et al., 2009).

S. alba is famous for analgesic effect due to the presence of salicin which have potent analgesic and anti-inflammatory properties. In this study significant antinociceptive effect was produced by the leaf extract of *S. alba* at doses of 50 mg/kg (66.45%) and 100 mg/kg (78.98%). Similarly, significant antinociceptive effect was also produced by the gold nanoparticles, but at much lower doses compared to that of leaf extract i.e. 72.87% and 80.76% at 5 and 10 mg/kg respectively. Moreover, the *S. alba* leaves extract (50 and 100 mg/kg) as well as the gold nanoparticles (5 and 10 mg/kg) produced significant muscle relaxant effect in both chimney and traction tests. These results suggest that the gold nanoparticles possess antinociceptive and muscle relaxant properties comparable to the leaves extract but at much lower doses. No sedative effect was produced by both *S. alba* leaves extract and its gold nanoparticles. A natural product having analgesic as well as muscle relaxant properties is beneficial as in majority of cases pain is usually accompanied with muscle stretching for which muscle relaxants are mostly prescribed along with analgesics. Pain and inflammation can result in unrelenting symptoms, misery, stress and sometimes disablement for the sufferer. Inflammation is the response to an injurious stimulus that can evoked by a wide variety of noxious agents. The classic inflammatory response includes warmth, pain, redness and swelling. Many mechanisms and mediators are involved in the promotion of the inflammatory process. Prostaglandins are important mediators of inflammation, fever and pain. They are synthesized by the constitutive enzyme, cyclooxygenase-1 (COX-1), and its isoform enzyme COX-2, which is induced in peripheral tissues by cytokines, growth factors and other inflammatory stimuli. Although in some situations prostaglandins contribute to pain by directly activating nociceptors, they are generally considered to be sensitizing agents. Prostaglandins increase the levels of cyclic AMP and may enhance nociceptor sensitization by reducing the activation threshold for TTX-R sodium channels via a protein kinase A pathway. They sensitize primary afferent neurons to bradykinin and other mediators and are likely to be involved at multiple sites along the nociceptive pathway (Kidd and Urban, 2001). The beneficial effect of willow plant to ease pain and reduce inflammation has been attributed to the presence of salicin among other active components including polyphenols and flavonoids. The presence of salicylates in willow provided foundation for the discovery of aspirin, the acetylated form of salicylic acid which subsequently leads to the synthesis of other effective analgesic and anti-inflammatory drugs i.e. non-steroid anti-inflammatory drugs (NSAIDs). Aspirin and NSAIDs inhibit the activity of COXs which inhibit the formation of prostaglandins and therefore relieve inflammation, swelling, pain and fever (Vane and Botting, 2003).

Keeping in view the well-known ethno-medicinal use of *S. alba*, the use of its gold nanoparticles is far better than prescribing two synthetic drugs for musculoskeletal pain as each drug has its own side effects. Furthermore, gold is usually prescribed for various joints pain conditions (Panyala et al., 2009). This added advantage along with its own potent analgesic and muscle relaxant properties compared to the leaves extract and diclofenac sodium, greatly promotes the use of *S. alba* gold nanoparticles as replacement herbal therapy for the clinical management of different pain conditions. Nanotechnological strategies change a substance's properties and behavior in a biological environment and can potentiate the actions of plant extracts, promote sustained release of active ingredients, reduce the required dose, decrease side effects and improve activity (Bonifácio and da Silva, 2014). Drug delivery system fetched a novel drug delivery system, a novel approach to overcome the drawbacks of the traditional drug delivery systems (Ansari and Farha Islam, 2012). Green

nanotechnology greatly promotes the development of biological medicine and bioavailability enhancement of herbal drugs (Bhadoriya et al., 2011).

5. Conclusions

We have developed a green method to synthesize gold nanoparticles using the leaves extract of *S. alba* that act as both reducing and stabilizing agent by avoiding the use of hazardous and toxic solvents. The nanoparticles are mostly in the size of 50–80 nm. FTIR analysis indicates the possible involvement of amines, amides and aromatic groups in the reduction process and may act as capping agents. Phytochemicals capping the nanoparticles make them colloidally stable in different media like salt and in various pH solutions but were relatively less stable at elevated temperature as revealed from their UV–Vis absorption spectra. The good antifungal activity along with significant attenuation of pain as well muscle relaxant effect of gold nanoparticles can be potentially applied in various products such as topical preparations. The process for the synthesis of nanoparticles in large scale using *S. alba* leaves extract may have several advantages such as cost-effectiveness and compatibility for biomedical and pharmaceutical applications.

Acknowledgement

The authors gratefully acknowledge financial support from the Higher Education Commission of Pakistan.

References

Ansari, S., Farha Islam, M., 2012. Influence of nanotechnology on herbal drugs: a review. J. Adv. Pharm. Technol. Res. 3, 142–146.
Archer, J., 1973. Tests for emotionality in rats and mice. A review. Anim. Behav. 21, 205–235.
Arslan, O., 2001. Inhibition of bovine carbonic anhydrase by new sulfonamide compounds. Biochem. – Moscow 66, 982–983.
Bahram, M., Mohammadzadeh, E., 2014. Green synthesis of gold nanoparticles with willow tree bark extract: a sensitive colourimetric sensor for cysteine detection. Anal. Methods 6, 6916–6924.
Bhadoriya, S.S., Mangal, A., Madoriya, N., Dixit, P., 2011. Bioavailability and bioactivity enhancement of herbal drugs by "nanotechnology": a review. J. Curr. Pharm. Res. 8, 1–7.
Bonifácio, B.V., da Silva, P.B., 2014. Nanotechnology-based drug delivery systems and herbal medicines: a review. Int. J. Nanomed. 9, 1–15.
Boyanova, L., Gergova, G., Nikolov, R., Derejian, S., Lazarova, E., Katsarov, N., Mitov, I., Krastev, Z., 2005. Activity of Bulgarian propolis against 94 helicobacter pylori strains in vitro by agar-well diffusion, agar dilution and disc diffusion methods. J. Med. Microbiol. 54, 481–483.
Burygin, G., Khlebtsov, B., Shantrokha, A., Dykman, L., Bogatyrev, V., Khlebtsov, N., 2009. On the enhanced antibacterial activity of antibiotics mixed with gold nanoparticles. Nanoscale Res. Lett. 4, 794–801.
Chauhan, R.P., Gupta, C., Prakash, D., 2012. Methodological advancements in green nanotechnology and their applications in biological synthesis of herbal nanoparticles. Int. J. Bioassays 1, 6–10.
Dykman, L., Khlebtsov, N., 2012. Gold nanoparticles in biomedical applications: recent advances and perspectives. Chem. Soc. Rev. 41, 2256–2282.
El-Shemy, H.A., Aboul-Enein, A.M., Aboul-Enein, K.M., Fujita, K., 2007. Willow leaves' extracts contain anti-tumor agents effective against three cell types. PLoS One 2, e178.
Goyal, M., Nagori, B., Sasmal, D., 2009. Sedative and anticonvulsant effects of an alcoholic extract of *Capparis decidua*. J. Nat. Med. 63, 375–379.
Gupta, A.K., Gupta, M., 2005. Synthesis and surface engineering of iron oxide nanoparticles for biomedical applications. Biomaterials 26, 3995–4021.
Haiss, W., Thanh, N.T., Aveyard, J., Fernig, D.G., 2007. Determination of size and concentration of gold nanoparticles from UV–vis spectra. Anal. Chem. 79, 4215–4221.
Harbourne, N., Marete, E., Jacquier, J.C., O'Riordan, D., 2009. Effect of drying methods on the phenolic constituents of meadowsweet (*Filipendula ulmaria*) and willow (*Salix alba*). LWT-Food Sci. Technol. 42, 1468–1473.
Hosseinzadeh, H., Ramezani, M., Namjo, N., 2003. Muscle relaxant activity of *Elaeagnus angustifolia* L. fruit seeds in mice. J. Ethnopharmacol. 84, 275–278.
Jain, P.K., Huang, X., El-Sayed, I.H., El-Sayed, M.A., 2008. Noble metals on the nanoscale: optical and photothermal properties and some applications in imaging, sensing, biology, and medicine. Acc. Chem. Res. 41, 1578–1586.
Jensen, T.R., Malinsky, M.D., Haynes, C.L., Van Duyne, R.P., 2000. Nanosphere lithography: tunable localized surface plasmon resonance spectra of silver nanoparticles. J. Phys. Chem. B 104, 10549–10556.
Kidd, B., Urban, L., 2001. Mechanisms of inflammatory pain. Br. J. Anaesth. 87, 3–11.
Klasnja, B., Kopitovic, S., Orlovic, S., 2002. Wood and bark of some poplar and willow clones as fuelwood. Biomass Bioenergy 23, 427–432.
Kumar, V., Yadav, S.K., 2009. Plant-mediated synthesis of silver and gold nanoparticles and their applications. J. Chem. Technol. Biotechnol. 84, 151–157.
Lee, S.K., Mbwambo, Z., Chung, H., Luyengi, L., Gamez, E., Mehta, R., Kinghorn, A., Pezzuto, J., 1998. Evaluation of the antioxidant potential of natural products. Comb. Chem. High Throughput Screen. 1, 35–46.
Levard, C., Hotze, E.M., Lowry, G.V., Brown Jr, G.E., 2012. Environmental transformations of silver nanoparticles: impact on stability and toxicity. Environ. Sci. Technol. 46, 6900–6914.
Mahdi, J., Mahdi, A., Bowen, I., 2006. The historical analysis of aspirin discovery, its relation to the willow tree and antiproliferative and anticancer potential. Cell Prolif. 39, 147–155.
Muhammad, N., Saeed, M., Khan, H., 2012. Antipyretic, analgesic and anti-inflammatory activity of *Viola betonicifolia* whole plant. BMC Complement Altern. Med. 12, 59.
Muhammad, N., Saeed, M., Khan, H., Haq, I., 2013. Evaluation of n-hexane extract of *Viola betonicifolia* for its neuropharmacological properties. J. Nat. Med. 67, 1–8.
Murphy, C.J., Gole, A.M., Hunyadi, S.E., Stone, J.W., Sisco, P.N., Alkilany, A., Kinard, B.E., Hankins, P., 2008. Chemical sensing and imaging with metallic nanorods. Chem. Commun., 544–557
Nel, A.E., Mädler, L., Velegol, D., Xia, T., Hoek, E.M., Somasundaran, P., Klaessig, F., Castranova, V., Thompson, M., 2009. Understanding biophysicochemical interactions at the nano–bio interface. Nat. Mater. 8, 543–557.
Panyala, N.R., Peña-Méndez, E.M., Havel, J., 2009. Gold and nano-gold in medicine: overview, toxicology and perspectives. J. Appl. Biomed. 7, 75–91.
Sadowski, Z., 2010. Biosynthesis and application of silver and gold nanoparticles. In: Perez, D.P. (Ed.), Silver Nanoparticles. InTech, pp. 257–276.
Sathishkumar, G., Gobinath, C., Karpagam, K., Hemamalini, V., Premkumar, K., Sivaramakrishnan, S., 2012. Phyto-synthesis of silver nanoscale particles using *Morinda citrifolia* L. and its

inhibitory activity against human pathogens. Colloid Surf. B 95, 235–240.
Shankar, S.S., Rai, A., Ahmad, A., Sastry, M., 2004. Rapid synthesis of Au, Ag, and bimetallic Au core–Ag shell nanoparticles using Neem (*Azadirachta indica*) leaf broth. J. Colloid Interface Sci. 275, 496–502.
Song, J.Y., Kim, B.S., 2009. Rapid biological synthesis of silver nanoparticles using plant leaf extracts. Bioprocess Biosyst. Eng. 32, 79–84.
Stankus, D.P., Lohse, S.E., Hutchison, J.E., Nason, J.A., 2010. Interactions between natural organic matter and gold nanoparticles stabilized with different organic capping agents. Environ. Sci. Technol. 45, 3238–3244.
Sumi, S.W., Nippon Rinsho, Y., 1996. Jpn. J. Clin. Med. 54, 3226–3229.
Sun, Y., Xia, Y., 2002. Increased sensitivity of surface plasmon resonance of gold nanoshells compared to that of gold solid colloids in response to environmental changes. Anal. Chem. 74, 5297–5305.
Thakkar, K.N., Mhatre, S.S., Parikh, R.Y., 2010. Biological synthesis of metallic nanoparticles. Nanomed.: Nanotechnol. Biol. Med. 6, 257–262.
Uddin, G., Rauf, A., 2012. In-vitro antimicrobial profile of *Pistacia integerrima* galls stewar. Middle-East J. Med. Plant. Res. 1, 36–40.
Vane, J.R., Botting, R.M., 2003. The mechanism of action of aspirin. Thromb. Res. 110, 255–258.
Villanueva-Ibáñez, M., Yañez-Cruz, M.G., Álvarez-García, R., Hernández-Pérez, M.A., Flores-González, M.A., 2015. Aqueous corn husk extract – mediated green synthesis of AgCl and Ag nanoparticles. Mater. Lett. 152, 166–169.
Vorkapic, D., Matsoukas, T., 1998. Effect of temperature and alcohols in the preparation of titania nanoparticles from alkoxides. J. Am. Ceram. Soc. 81, 2815–2820.
Wang, Y., He, X., Wang, K., Zhang, X., Tan, W., 2009. *Barbated Skullcup* herb extract-mediated biosynthesis of gold nanoparticles and its primary application in electrochemistry. Colloid Surf. B 73, 75–79.
Zhu, M., Nie, G., Meng, H., Xia, T., Nel, A., Zhao, Y., 2012. Physicochemical properties determine nanomaterial cellular uptake, transport, and fate. Acc. Chem. Res. 46, 622–631.

Please cite this article in press as: Islam, N.U. et al., Green synthesis and biological activities of gold nanoparticles functionalized with *Salix alba*. Arabian Journal of Chemistry (2015), http://dx.doi.org/10.1016/j.arabjc.2015.06.025